Available online at www.eccomasproceedia.org
Eccomas Proceedia COMPDYN (2023) 2566-2580

ECCOMAS
Proceedia

COMPDYN 2023
9th ECCOMAS Thematic Conference on
Computational Methods in Structural Dynamics and Earthquake Engineering
M. Papadrakakis, M. Fragiadakis (eds.)
Athens, Greece, 12-14 June 2023

SEISMIC POUNDING OF TYPICAL REINFORCED CONCRETE BUILDINGS SUBJECT TO SOIL STRUCTURE INTERACTION EFFECTS

Ibrahim OZ[1], Kaan KAATSIZ[2]

[1] Ibrahim OZ
Kirsehir Ahi Evran University, 40100 Kirsehir, Turkey
e-mail: ibrahim.oz@ahievran.edu.tr

[2] Kaan KAATSIZ
Kirsehir Ahi Evran University, 40100 Kirsehir, Turkey
e-mail: kaan.kaatsiz@ahievran.edu.tr

Abstract

Adjacent structures are often not sufficiently separated due to the land costs of the construction areas in densely populated regions. Moreover, existing structures located in a block may have zero or insufficient distance in between due to architectural or economical constraints despite current seismic provisions. This study aims to evaluate the collision behavior of typical reinforced concrete structures by considering the effects of Soil Structure Interaction (SSI). Seismic response of 2D reinforced concrete frame models having 4 and 6 storeys are evaluated for two different soil conditions. The direct method is chosen to include SSI effects. Inelastic time history analyses are performed under ten strong ground motion records. Story shear forces, pounding forces, and story drifts are compiled from analyses and compared for two different soil conditions. Results indicate that the seismic response of typical reinforced concrete structures in terms of storey drifts and floor accelerations changes considerably due to pounding induced collision and inclusion of SSI effects in the dynamic analyses.

Keywords: Soil-Structure Interaction, Pounding, Seismic Response, Nonlinear Analysis.

doi: 10.7712/120123.10583.20946

1 INTRODUCTION

Although codes and regulations [1, 2, 3] specify the minimum seismic gap between adjacent structures, these limits often ignored in densely populated residential areas due to factors such as high land costs or architectural concerns. Seismic gaps can be reduced or adjacent structures might even be built with no separations. Even there are regulations and provisions regulating the gap between adjacent buildings, these gaps may not be in accordance with the specified conditions if not properly controlled during construction. Seismic provisions such as Turkish Earthquake Code (TBEC-2018) specify analysis guidelines considering the building stand as free, stand-alone state. The structures under design are not differentiated whether they have adjacent existing buildings on site, or not. However, structures with insufficient seismic gap in between exhibit different displacement response during earthquake action due to their different dynamic properties (vibration periods etc.). This may result in adjacent structures colliding with each other. Previous studies investigating the seismic behavior of adjacent structures have carried out studies using fixed-support models [4, 5, 6, 7] by ignoring the soil-structure interaction (SSI). However, it is known that the SSI effects can amplify the seismic response of the superstructure [8, 9, 10].

Pounding effects of reinforced concrete (RC) structures modeled via soil structure interaction (SSI) refer to the impact and collision forces that occur between adjacent structures during an earthquake. These forces can result in severe damage, structural failure, or even collapse of the structures involved [11]. The pounding behavior are affected by several factors such as the dynamic response of the structures, soil shear wave velocity and the nature of the ground motion. Understanding and mitigating the pounding effects of RC structures with included SSI effects is crucial in the design and construction of resilient and safe buildings in earthquake prone regions. It involves specialized analysis techniques, structural design measures, and the implementation of appropriate building codes and standards.

This study aims to evaluate the collision behavior of low and mid-rise adjacent RC structures modeled with SSI. In accordance with this purpose, 2D frame models having 4 and 6 storeys are analyzed considering two different soil conditions with soil shear wave velocities of 198 m/s and 398 m/s respectively. The direct method, which is structure and soil medium are modeled and analyzed at the same time, is chosen to consider SSI effects. Seismic gap between the adjacent structures is determined as described in TBEC-2018. To avoid soil amplifications for twice during considered analyses ground motion records are chosen from soils which have shear wave velocity greater than 1000 m/s.

No analytical model with fixed support conditions was used during the analysis, and all analyzes were performed by taking into account the SSI effects. Response evaluation such as comparison of the analysis results of the model of the 4 storey building on V_{s30} 198m/s soil with those of the pounding case of the 4 and 6 storey structures on V_{s30} 198m/s soil were carried out.

2 STRUCTURAL MODELS AND SSI

The 4 and 6 storey structures considered in the study are the type of buildings representing the general Turkish building stock [12]. The two bays in the X direction of the buildings, which are modeled as a two-dimensional frame, are 5 meters in span and the floor height is 3 meters in all stores. In order to represent the nonlinear behavior of structures, fiber hinges that directly consider material properties are used in beam and column end regions. The non-linear stress-strain curves of the reinforcement and concrete material models employed in the hinges are shown in Fig. 1.

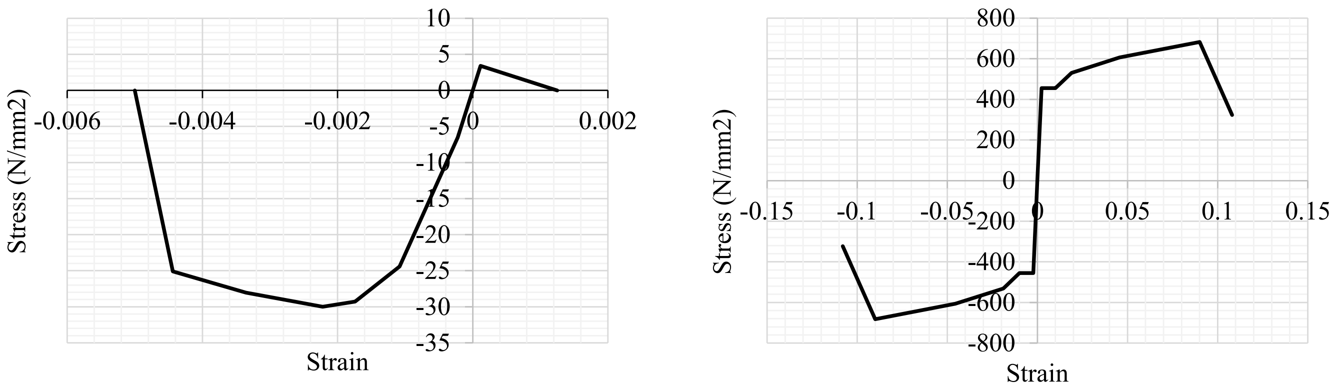

Figure 1. Material properties of concrete (left) and reinforcement (right).

All columns are 60 cm by 30 cm with the strong axis is located in direction of the earthquake excitation. The reinforcement layouts of columns and beams are shown in Fig. 2Crack section stiffness is defined to elastic portions reinforced concrete elements as 0.35*I for beams*, and 0.7*I* for columns.

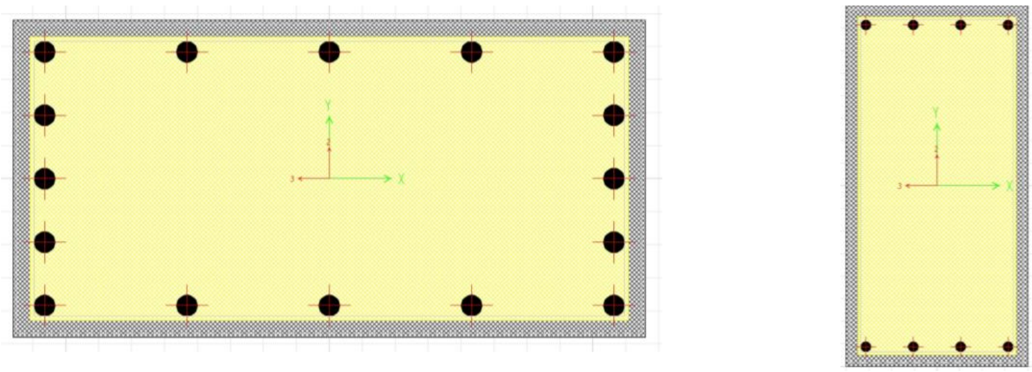

Figure 2. Reinforcement layouts of columns (left) and beams (right).

In Fig.3 a schematic illustration of the x-z plane views of the 4- and 6-storey frame models are given. The capacity curves of the examined buildings obtained from nonlinear pushover analyses are shown in Fig. 4. When the capacity curves are examined in detail, it can be stated that the buildings inspected in the study in terms of lateral strength ratio and drift ratio capacities represent the relatively better portion of the Turkish building stock in terms of ductile behavior and base shear capacity [12].

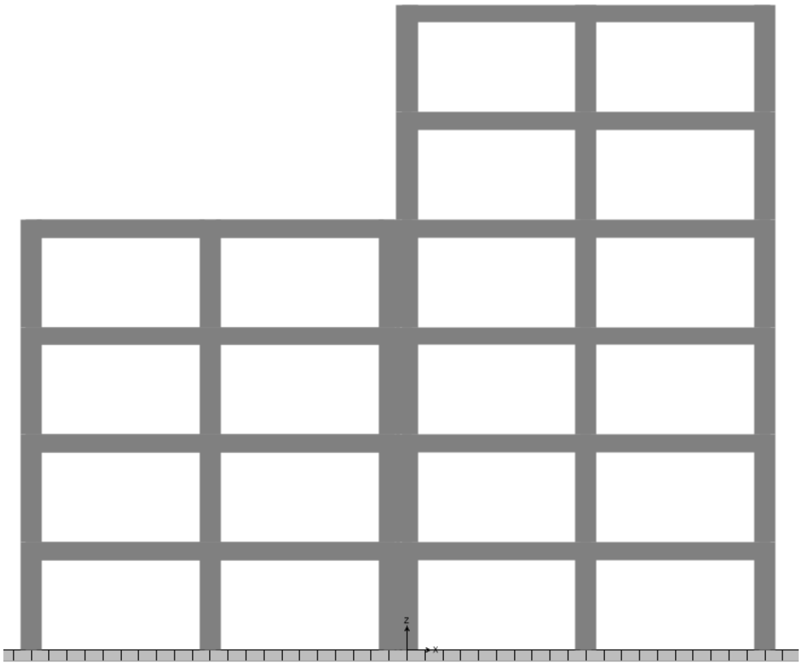

Figure 3. X-Z plan views of structures

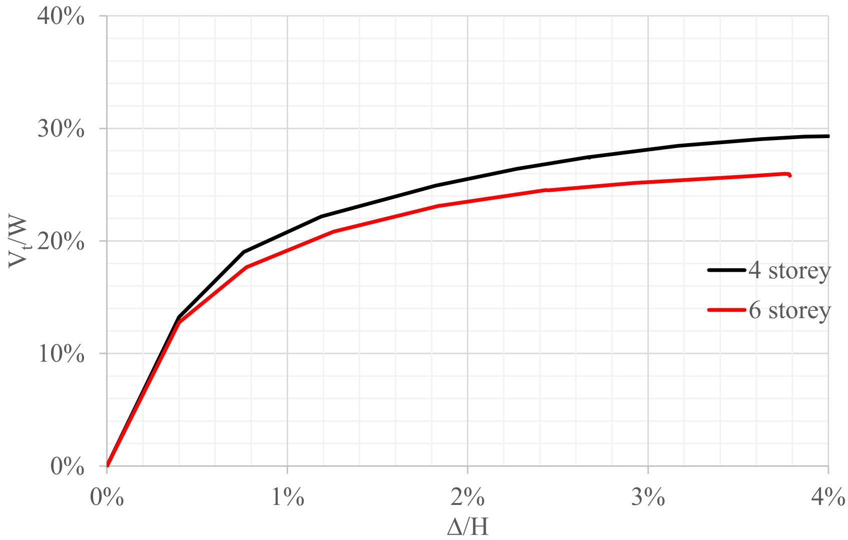

Figure 4. Unitless capacity curves of examined structures.

As mentioned before, "Direct Method" [13, 14] was preferred while considering SSI effects in the study. The soil medium is modeled in 2D with solid elements and meshed two meters in horizontal by 1 meter in vertical. In the near field regions of the superstructure, mesh dimensions have been reduced to 0.5 meters in both directions [11]. The soil medium is assumed to be not homogeneous in vertical [15]. Therefore 31 different types of soil material defined for a total depth of 35 meters. Rather than using viscous boundaries which are employed to exclude waves reflected back from the soil medium into the analysis domain, the soil medium is extended to 500 meters in horizontal direction. Soil profiles are are determined by using the non-commercial software DEEPSOIL [16] and shown in Fig 5 and Fig. 6 for V_{s30}=398 m/s and V_{s30}=198 m/s respectively.

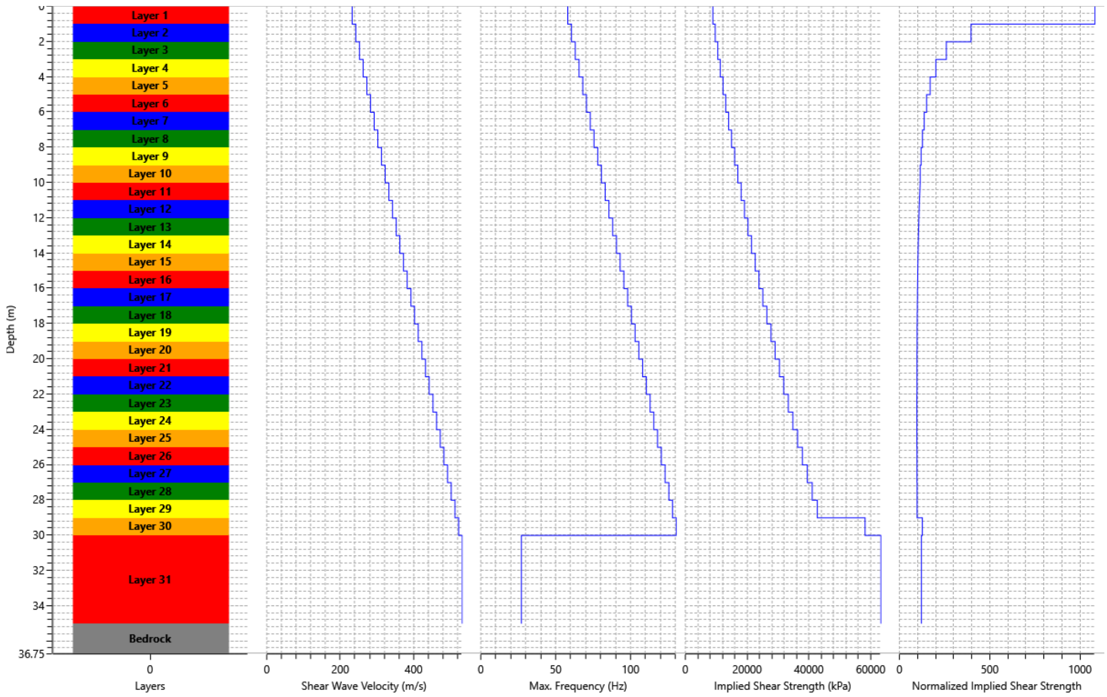

Figure 5. Soil profile of V_{s30}=398 m/s.

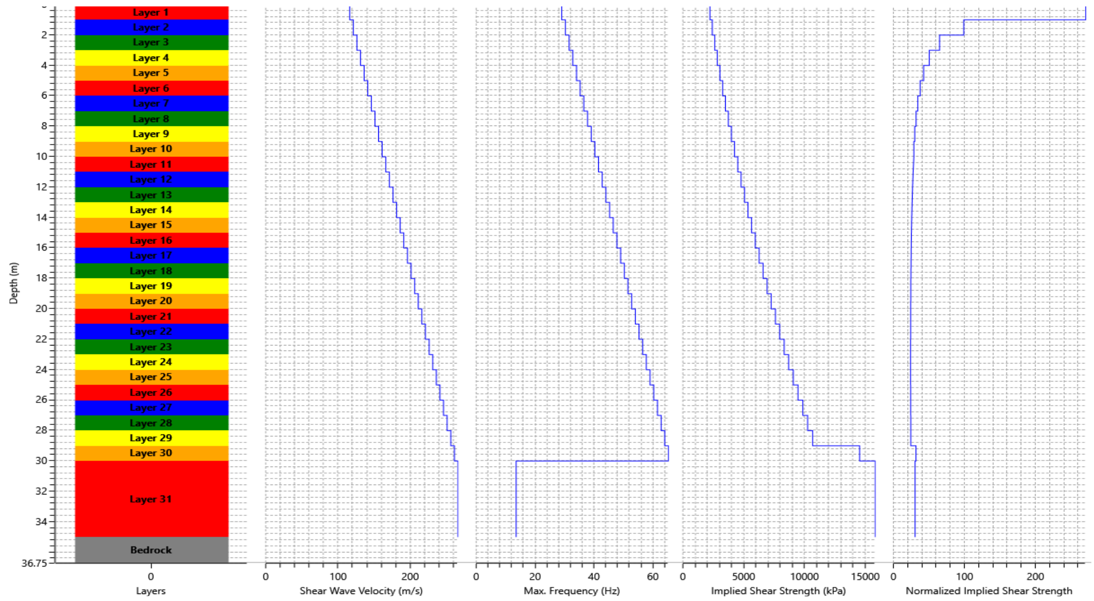

Figure 6. Soil profile of Vs30=198 m/s.

While considering the seismic gap between adjacent structures, TBEC-2018 specifications has been taken into account. According to the specification, adjacent structures shall have 3 cm gap for the first 3 m and 1 cm should be added to this gap for every other 3 m. Therefore, the seismic gap for 4 and 6 storey structures is considered as 6 cm for pounding cases. The equation is given in Eq. (1).

$$d_2=(H-6)/3+3 \tag{1}$$

Two dimensional reinforced concrete nonlinear structure models were used in this study. It is known that if the storey diaphragms at different levels between adjacent structures, calculations and modeling of pounding behavior differs from the structures having same level storey diaphragms. In this study, pounding behavior is considered between adjacent structures with same storey heights of 3m. Hence, storey diaphragms of considered structures are at the same level for each storey. If adjacent structures have the same structural properties (i.e., same vibration periods) no collisional behavior is expected. However, is not likely to happen in reality.

Collision behavior is simulated as the subjected nodes of two adjacent structures come into contact. Linear visco-elastic connection model is used in modelling of the gap elements [11, 17].In order to model this behavior, linear - viscoelastic gap element is used at storey levels between two structures. Kelvin-Voigt model [18] is the most used model to define gap element properties for pounding problems [11]. Therefore, it is utilized in this study and respective parameters are computed. In Eq. (2) and Eq. (3) stiffness coefficient is shown by KL and the damping coefficient is shown by CL, where *e* is the coefficient of energy efficiency. KL value is taken as 9350 t/m and the e value is taken as 0.65 [21]. The stiffness of gap element (KG) is considered 100 times of KL to prevent convergence errors. A schematic illustration of gap elements is shown in Fig.7, a representative figure of the pounding model is shown in Fig 7.

$$C_L = 2\xi\sqrt{K_L\frac{m_1 m_2}{m_1 + m_2}} \tag{2}$$

$$\xi = -\frac{\ln(e)}{\sqrt{\pi^2 + \ln(e)^2}} \tag{3}$$

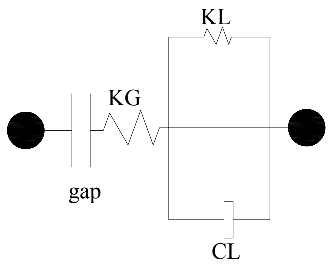

Figure 7. Representation of the gap element.

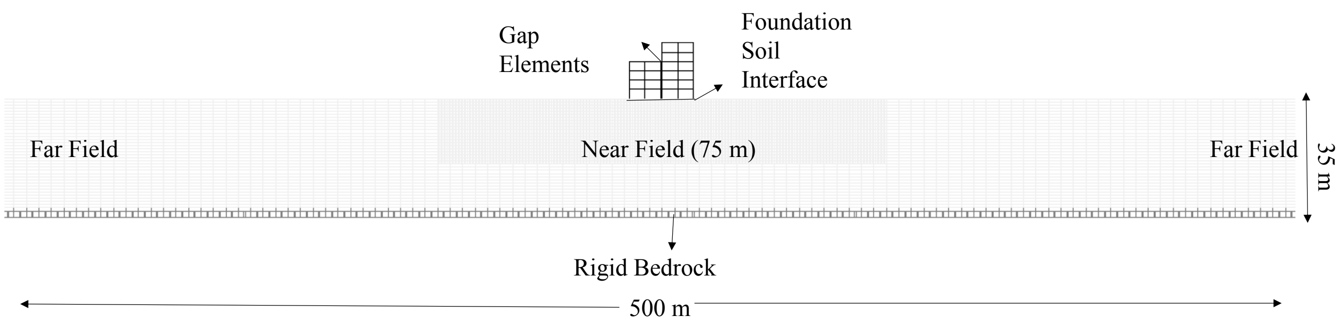

Figure 8. Schematic illustration of 2-D SSI pounding model.

3 GROUND MOTION RECORDS

The structures that are inspected within the scope of the study were subjected to non-linear time history analyses under 10 strong ground motion records. It is known that the soil amplifications vary according to the soil type and generally increase as the soil shear wave velocity decreases [19]. For this reason, instead of considering the ground amplifications of both the soil where the station is located and the soil medium that surrounding the inspected structures, attention was paid to ensure that the shear wave velocity of the soil where the station located where the ground motion record is obtained is greater than 1000 m/s [15, 16, 19]. Thus, the SSI pounding models analyzed were only exposed to the amplifications of the soil environment included in the model. The average spectrum of the ground motions and the free vibration periods of the investigated buildings are shown in Fig. 9, and in Table 1 detailed information of the selected ground motions from PEER NGA [20] database are given.

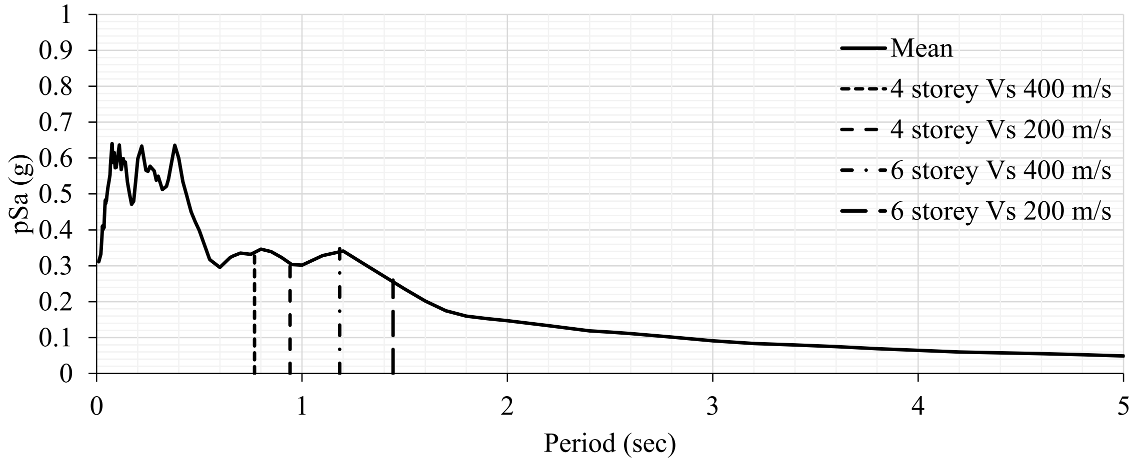

Figure 9. Mean spectrum and the free vibration periods of investigated structures.

Table 1. The ground motion records subjected the study.

Record Sequence Number (PEER NGA)	**Earthquake Name**	**Year**	**Magnitude**	**Vs30 (m/sec)**
77	San Fernando	1971	6.61	2016.13
765	Loma Prieta	1989	6.93	1428.14
795	Loma Prieta	1989	6.93	1249.86
804	Loma Prieta	1989	6.93	1020.62
879	Landers	1992	7.28	1369.00
1011	Northridge-01	1994	6.69	1222.52
1108	Kobe Japan	1995	6.90	1043.00
1257	Chi-Chi Taiwan	1999	7.62	1525.85
1366	Chi-Chi Taiwan	1999	7.62	1010.40
3799	Hector Mine	1999	7.13	1015.88

4 ANALYSIS RESULTS AND CONCLUSIONS

When collision behavior occurs between two adjacent buildings, the seismic behavior of both buildings under ground motion can be affected by the discussed interactions. While the displacement demand in the collision direction may decrease for both structures, the displacement demands of the structures in the free direction may increase as a result of the momentum behavior caused by the collision [11].

In Fig. 10, the roof displacement time series for the free and pounding directions and the link forces occurring in the floors are given for the soil condition with the shear wave velocity of 198 m/s for 4 and 6 storey buildings. Results are given both in the non-pounding and pounding conditions for the record sequence number 1257 (Chi-Chi Taiwan). Upon inspection of the link forces in this figure, it is seen that the collision occurred not only at the 4th storey, but at the other stories as well. Therefore, it can be concluded that the additional storey shear forces and displacement demands occurring due to collision behavior should be considered for both in the design, and evaluation of the seismic behavior of existing buildings.

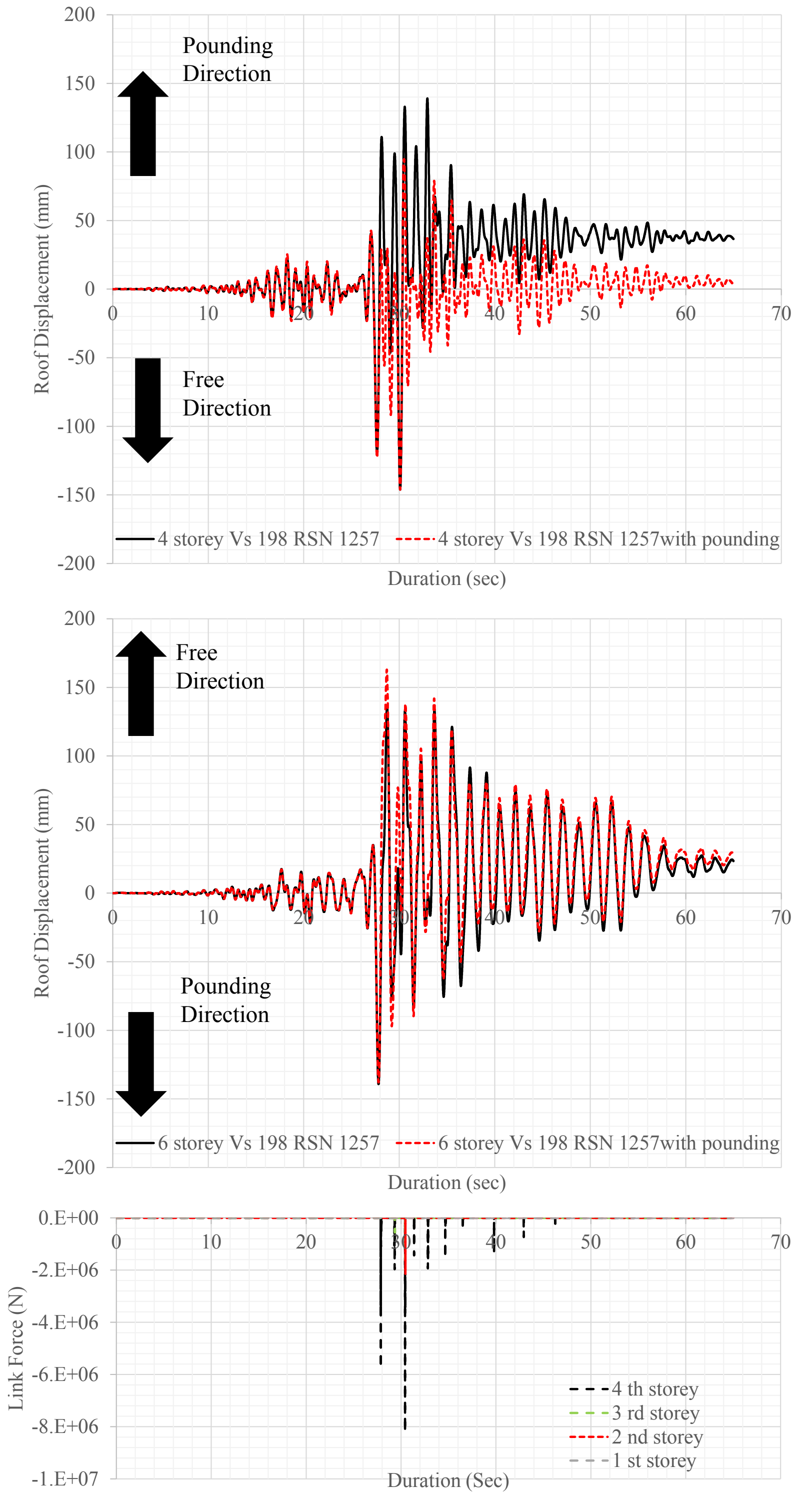

Figure 10. Displacement-time series of the roofs and link forces for the record RSN 1257.

The maximum and minimum displacement demands obtained for each floor are compiled from the nonlinear time history analyses conducted under 10 strong ground motion records and their averages are given in Table 2 for 4-storey structures, and in Table 3 for 6 storey structures.Table 2. Average of maximum and minimum storey demands of 4 storey structure (units in mm).

Storey No	4 storey V_{s30}=198 m/s				4 storey V_{s30}=398 m/s			
	Stand Alone Case Pounding Direction	Pounding Case Pounding Direction	Stand Alone Case Free Direction	Pounding Case Free Direction	Stand Alone Case Pounding Direction	Pounding Case Pounding Direction	Stand Alone Case Free Direction	Pounding Case Free Direction
4	145.46	106.25	-169.88	-170.77	122.81	99.64	-106.38	-107.95
3	78.69	62.25	-94.85	-91.58	78.44	66.66	-66.32	-67.20
2	49.81	47.02	-48.86	-47.26	45.39	41.41	-37.47	-36.98
1	118.53	87.36	-140.77	-141.09	98.42	76.32	-87.60	-88.39

The analysis results for the soil with a shear wave velocity of 198m/s in the 4-storey building model show that the average of the roof displacement demands in the collision direction is reduced by 27% for the pounding condition. The same rate was calculated as 33% for the 3rd floor, 5% for the 2nd floor and 27% for the 1st floor. In the free direction for the same model, it is seen that there is a slight increase in displacement demand on the roof, 2nd floor and 1st floor, and a slight decrease in the displacement demand on the 3rd floor. For the model with a shear wave velocity of 398m/s, the results of the 4-storey buildings are similar for the soil with a shear wave of 198m/s. While the displacement demand of the structure is severely restricted in the collision direction (nearly 30%), a slight increase is observed in the free direction.

Table 2. Average of maximum and minimum storey demands of 6 storey structure.

Storey No	6 storey V_{s30}=198 m/s (mms)				6 storey V_{s30}=398 m/s (mms)			
	Stand Alone Case Pounding Direction	Pounding Case Pounding Direction	Stand Alone Case Free Direction	Pounding Case Free Direction	Stand Alone Case Pounding Direction	Pounding Case Pounding Direction	Stand Alone Case Free Direction	Pounding Case Free Direction
6	-170.58	-177.74	197.04	210.00	-125.58	-122.17	172.65	172.05
5	-150.24	-158.10	175.85	190.60	-117.72	-113.86	153.74	156.84
4	-122.78	-130.20	145.05	162.34	-108.33	-104.70	137.20	139.63
3	-73.12	-74.17	92.47	100.33	-60.54	-59.45	72.94	71.77
2	-56.25	-56.61	66.16	68.96	-32.17	-29.57	39.35	37.42
1	-96.89	-100.84	115.43	129.35	-90.42	-87.50	108.78	111.65

The averages of the maximum and minimum of the displacement demands for 6-storey buildings show that the displacement demands in the pounding direction increase slightly for the soil with a shear wave of 198 m/s, and decrease slightly for the soil with a shear wave velocity of 398 m/s. However, the averages results obtained for the soil condition with a shear wave velocity of 198m/s showed that the drift demands of the 6-storey building in the free direction increased by around 5%. Table 2 and Table 3 show that the pounding effects affect the short-period building in particular, but the longer period building is less affected- The examined building group shows that the displacement demands of the buildings are dramatically reduced (in some cases almost 40%) in pounding direction, while the demand may increase relatively less (%10), in the free direction.

All drift demands obtained from nonlinear dynamic analyses are compiled and sorted in an ascending order and plotted in logarithmic scale. Thus, the displacement demand values given as average for buildings can be presented as a single plot for all acceleration records. This plot in fact yields the probability of exceedance of a drift demand for all building types. In Fig. 11

these probabilities of exceedances given at the roof of the 4 storey structure for different analysis cases.

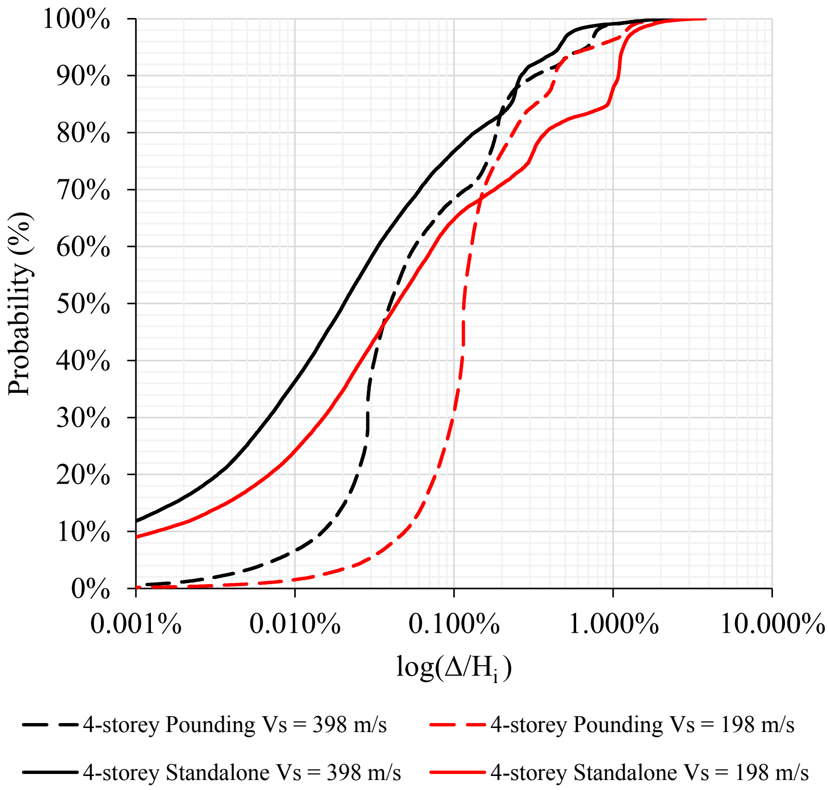

Figure 11. Probabilities of exceedances of drift ratios of the 4-storey structure.

The probabilities of exceedances of the roof displacement demands obtained from the different analyses of the 4-story model show that no significant difference the pounding and non-pounding conditions for the soil condition with the shear wave velocity of 398m/s. However, as the soil shear wave decreases, the results show that the roof displacement values of the 4-storey building are limited by the pounding behavior, and there is a significant decrease in values corresponding probability of exceedance to 10%.

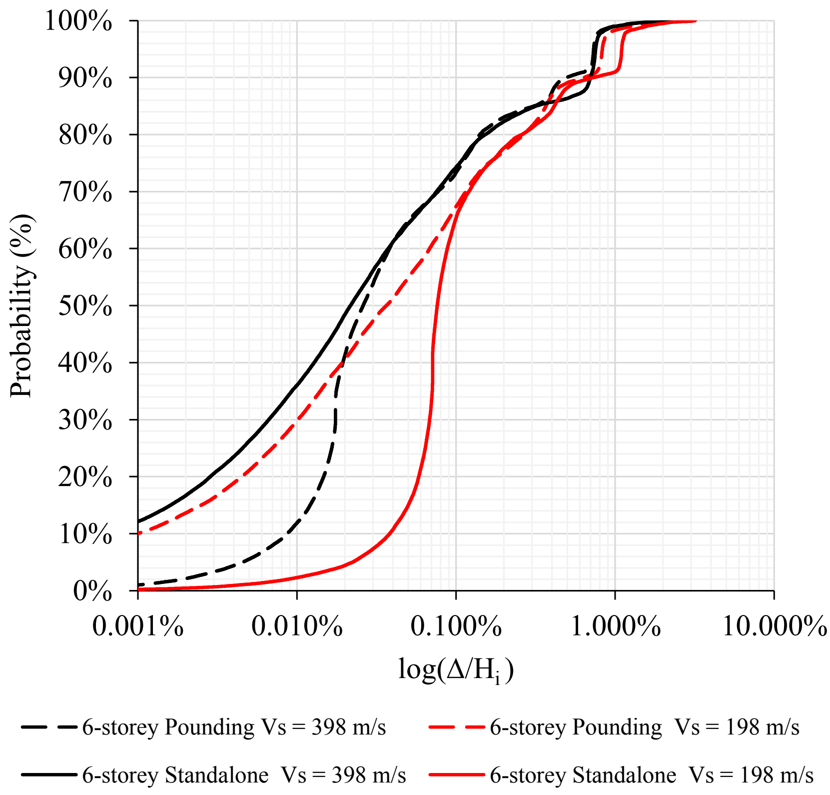

Figure 12. Probabilities of exceedances of drift ratios of the 6-storey structure.

The probabilities of exceedance of drift limits for 6 story building analyses are given in Fig. 12. It is observed that the pounding effects reduce the roof drifts in the 6-storey building, although reduction of the drift rates of 6-storey structure is relatively less than the 4-storey building. Although the drift values of the roof are given in the graph, the last floor where the building is exposed to pounding effects is the 4th floor of the 6-storey building. Therefore, the probabilities of exceedance of the 4th floor drifts are given separately in Fig. 13.

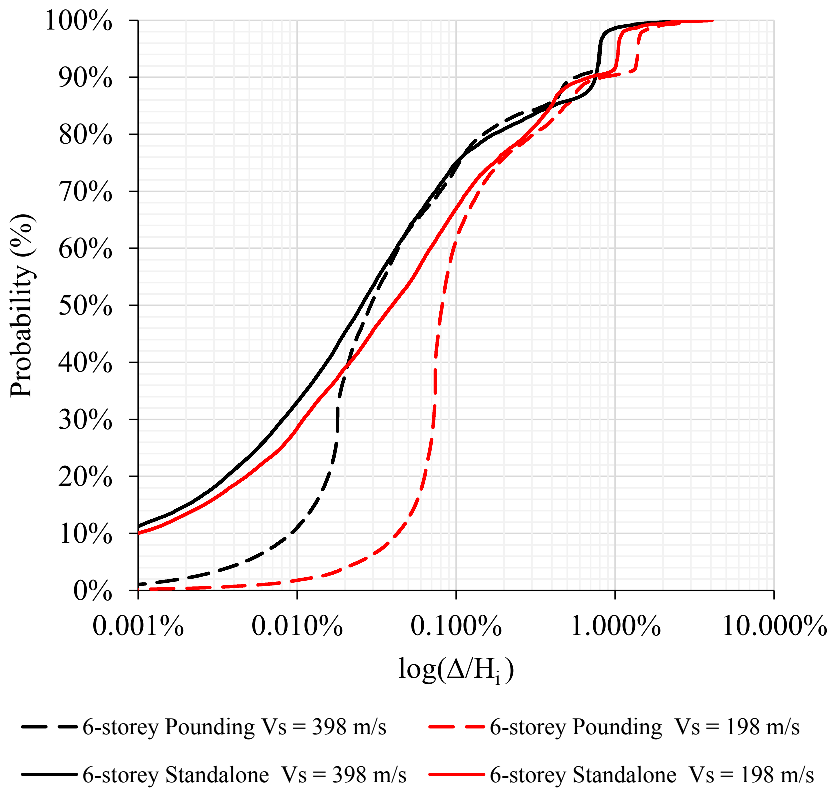

Figure 13. Probabilities of exceedances of drift ratios of the 4th storey of 6 storey structure.

On the 4th storey of the 6-storey structure, the displacement demands that corresponding to the probability of exceedance of 10% increase with the pounding effects about 50%. Fig. 12 and Fig. 13 show that although the roof displacement demands of the building may decrease with the pounding effects however, the displacement demands at the pounding floor may increase.

In addition to the displacement demands, the ratios of the accelerations occurring in the floors in the pounding state, and the floor accelerations occurring in the non-pounding state are also investigated. In Table 3, means of the maximum of the floor acceleration ratios of the pounding state and the non-pounding state are given, for each direction and both cases ($a_{pound}/a_{wopound}$).

Table 3. Ratios of the floor accelerations of investigated states.

Storey	4 Storey Vs 198		4 Storey Vs 398		6 Storey Vs 198		6 Storey Vs 398	
No	Free Direction	Pounding Direction	Free Direction	Pounding Direction	Pounding Direction	Free Direction	Pounding Direction	Free Direction
6					1.05	1.22	1.00	1.09
5					1.33	1.95	1.23	1.56
4	5.39	1.56	2.51	1.22	4.27	9.40	2.07	3.44
3	2.76	1.15	1.11	1.01	1.21	3.18	1.36	1.55
2	1.56	1.22	1.12	1.06	1.16	1.87	1.40	1.33
1	4.38	1.05	1.85	1.03	1.48	5.58	1.06	1.83

Table 3 shows the averages of $a_{pound}/a_{wopound}$ values. These ratios show that pounding effects increase the acceleration demands in the all storeys of buildings for both directions. However, especially at 1st and 4th floors, the acceleration demands increases are more significant on the free direction which can be explained by the momentum effects [11].

5 CONCLUSIONS

This study investigates the pounding effect on seismic behavior of 2D frame structures modeled with inclusion of SSI effects.. The selected frame systems represents the existing Turkish building stock. Nonlinear time history analyses conducted under 10 strong ground motion records. The important outcomes for investigated cases from the study are given as follows:

- The results for the investigated buildings show that pounding behavior can occur not only at the collision floor but also at other floors.
- In general, pounding effects are restricting the displacements in pounding direction. On the other hand, these effects increase the displacement demands in the free direction.
- The probabilities of exceedance corresponding to the drift ratio demands of the top stories indicate that the top story displacement demands of the 4-storey structures is reduced considerably. The 6-storey structure, on the other hand, is less affected than the 4-storey structure although there was a slight decrease in the roof displacement demand.
- Acceleration demands are found to increase significantly in both direction such that it can reach up to 5 times for 4 storey structures, and 9 times for 6 storey structures in free direction.
- It should be noted that the results of this study obtained from 2d reinforced concrete structures with analyses conducted under individual ground motions. Further studies are to be performed to generalize the results for different types of structures.

REFERENCES

[1] Turkish Building Earthquake Code (TBEC). Principles for the Design of Buildings under Earthquake. Ankara, Turkey (in Turkish): Ministry of Interior Disaster and Emergency Management Presidency; 2018.

[2] International Building Code (IBC). International Code Council. USA: Virginia; 2018.

[3] European Committee for Standardization. 2004 Eurocode 8 (EC8).

[4] Mazza, F., & Labernarda, R. (2022). Effects of near fault acceleration and non - acceleration pulses on pounding between in plan irregular fixed base and base isolated buildings. *Structural Control and Health Monitoring*, **29(9),** e2992.

[5] Miari, M., Choong, K. K., & Jankowski, R. (2019). Seismic pounding between adjacent buildings: Identification of parameters, soil interaction issues and mitigation measures. *Soil Dynamics and Earthquake Engineering*, **121**, 135-150.

[6] Miari, M., Choong, K. K., & Jankowski, R. (2021). Seismic pounding between bridge segments: a state-of-the-art review. *Archives of Computational Methods in Engineering*, **28**, 495-504.

[7] Mahmoud, S., & Jankowski, R. (2010). Pounding-involved response of isolated and non-isolated buildings under earthquake excitation. *Earthquake and Structures*, **1(3)**, 231-252.

[8] Brunelli, A., De Silva, F., & Cattari, S. (2022). Site effects and soil-foundation-structure interaction: derivation of fragility curves and comparison with codes-conforming approaches for a masonry school. *Soil Dynamics and Earthquake Engineering*, **154**, 107125.

[9] Forcellini, D. 2020. "A resilience-based methodology to assess soil structure interaction on a benchmark bridge." *Infrastructures*, **5** (11): 1–14. Thomas Telford Ltd. https://doi.org/10.3390/infrastructures5110090.

[10] Forcellini, D. 2022. "The Role of Soil Structure Interaction on the Seismic Resilience of Isolated Structures." *Appl. Sci.,* **12 (19)**: 9626. Multidisciplinary Digital Publishing Institute. https://doi.org/10.3390/app12199626.

[11] Cayci, B. T., & Akpinar, M. (2021, December). Seismic pounding effects on typical building structures considering soil-structure interaction. *Structures* **Vol. 34**, pp. 1858-1871. Elsevier.

[12] Inel, M., Ozmen, H. B., & Bilgin, H. (2008). Re-evaluation of building damage during recent earthquakes in Turkey. *Engineering Structures*, **30(2)**, 412-427.

[13] El Hoseny, M., Ma, J., Dawoud, W., & Forcellini, D. (2023). The role of soil structure interaction (SSI) on seismic response of tall buildings with variable embedded depths by experimental and numerical approaches. *Soil Dynamics and Earthquake Engineering*, **164**, 107583

[14] Li, J., Zhou, L., Li, S., Lin, G., & Ding, Z. (2023). Soil–structure interaction analysis of nuclear power plant considering three-dimensional surface topographic irregularities based on automatic octree mesh. *Engineering Structures*, **275**, 115161.

[15] Tzong, T. J., & Penzien, J. (1983). Hybrid modelling of soil-structure interaction in layered media. Berkeley, CA: Earthquake Engineering Research Center, University of California.

[16] Hashash, Y., Park, D. and Tsai, C. C., Philips, C. and Groholski, D.R. (2016), “DEEPSOIL - 1-D Wave Propagation Analysis Program for Geotechnical Site Response Analysis of Deep Soil Deposits, Version 6.1”, Tutorial and User Manual, University of Illinois at Urbana Campaign.

[17] Farghaly Ahmed Abdelraheem. Seismic analysis of adjacent buildings subjected to double pounding considering soil–structure interaction. *Int J Adv Struct Eng* 2017; 9(1):51–62. https://doi.org/10.1007/s40091-017-0148-y.

[18] Roylance D. *Engineering viscoelasticity*, **vol 2139**. 2001, p. 1-37.

[19] Derghoum, R., & Derghoum, I. (2023). Nonlinear finite element analysis for seismic site amplification assessment of urban slopes showing surface geology and topography irregularities. *Soil Dynamics and Earthquake Engineering*, **166**, 107729

[20] Pacific Earthquake Engineering Center (PEER). PEER Ground Motion Database. Available online: https://ngawest2.berkeley.edu/

[21] Jankowski Robert. Non-linear viscoelastic modelling of earthquake-induced structural pounding. *Earthq Eng Struct Dyn* 2005;**34(6)**:595–611. https://doi.org/10.1002/(ISSN)1096-984510.1002/eqe.v34:610.1002/eqe.434.